Central Himalayan tree-ring isotopes reveal increasing regional heterogeneity and enhancement in ice-mass loss since the 1960s

Running title: Glacier dynamics of the central Himalaya

Nilendu Singh[1], Mayank Shekhar[2], Jayendra Singh[3], Anil K Gupta[4], Achim Bräuning[5*], Christoph Mayr[5], and Mohit Singhal[1]

[1]*Centre for Glaciology, Wadia Institute of Himalayan Geology, Dehradun 248001, India*
[2]*Birbal Sahni Institute of Palaeosciences, Lucknow 226007, India*
[3]*Wadia Institute of Himalayan Geology, Dehradun 248001, India*
[4]*Center for Oceans, Rivers, Atmosphere and Land Sciences, IIT Kharagpur 721302, India*
[5]*Institute of Geography, University of Erlangen-Nuremberg, Erlangen 91058, Germany*

*Corresponding Author: achim.braeuning@fau.de

The supplementary material consists of 6 figures, and 6 tables (all referred in the main text)
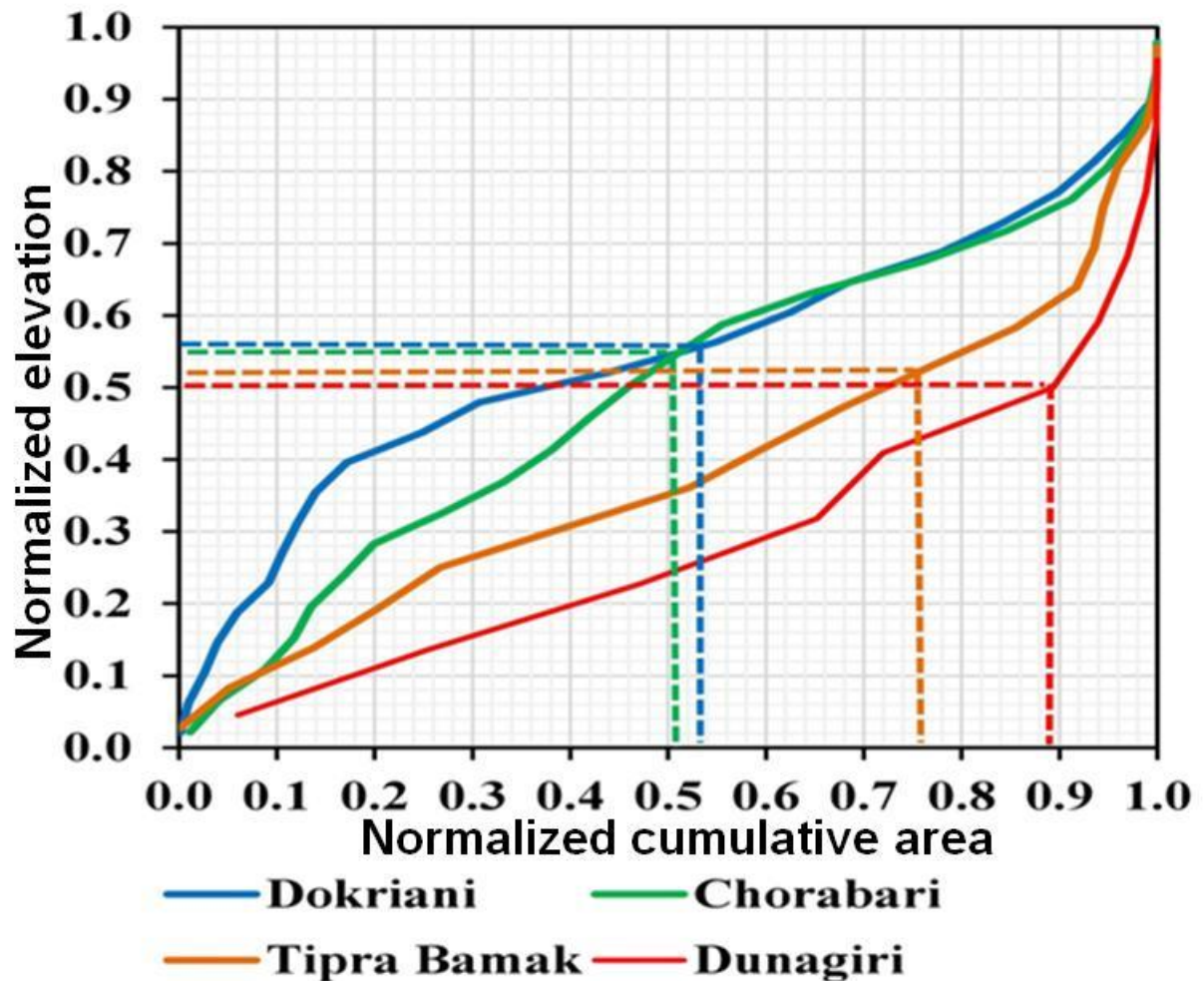
Figure S1. **Glacier hypsometry of four benchmark glaciers** (Dokriani: DOK; Chorabari: CHO; Tipra Bamak: TIP; and Dunagiri: DUN) of the Ganga Basin/WCH. The curve is convex for the DOK and CHO glaciers, while it was concave for the TIP and DUN glaciers. The dashed lines for each glacier were assigned the same colour as their corresponding hypsometric curve. The horizontal dashed lines are showing normalized snow line altitude (SLA) for each individual glacier while vertical lines indicate area at elevation similar to SLA. Hypsometric curves of these four glaciers are representative of the glaciers found in the central Himalaya (Garg et al., 2017).
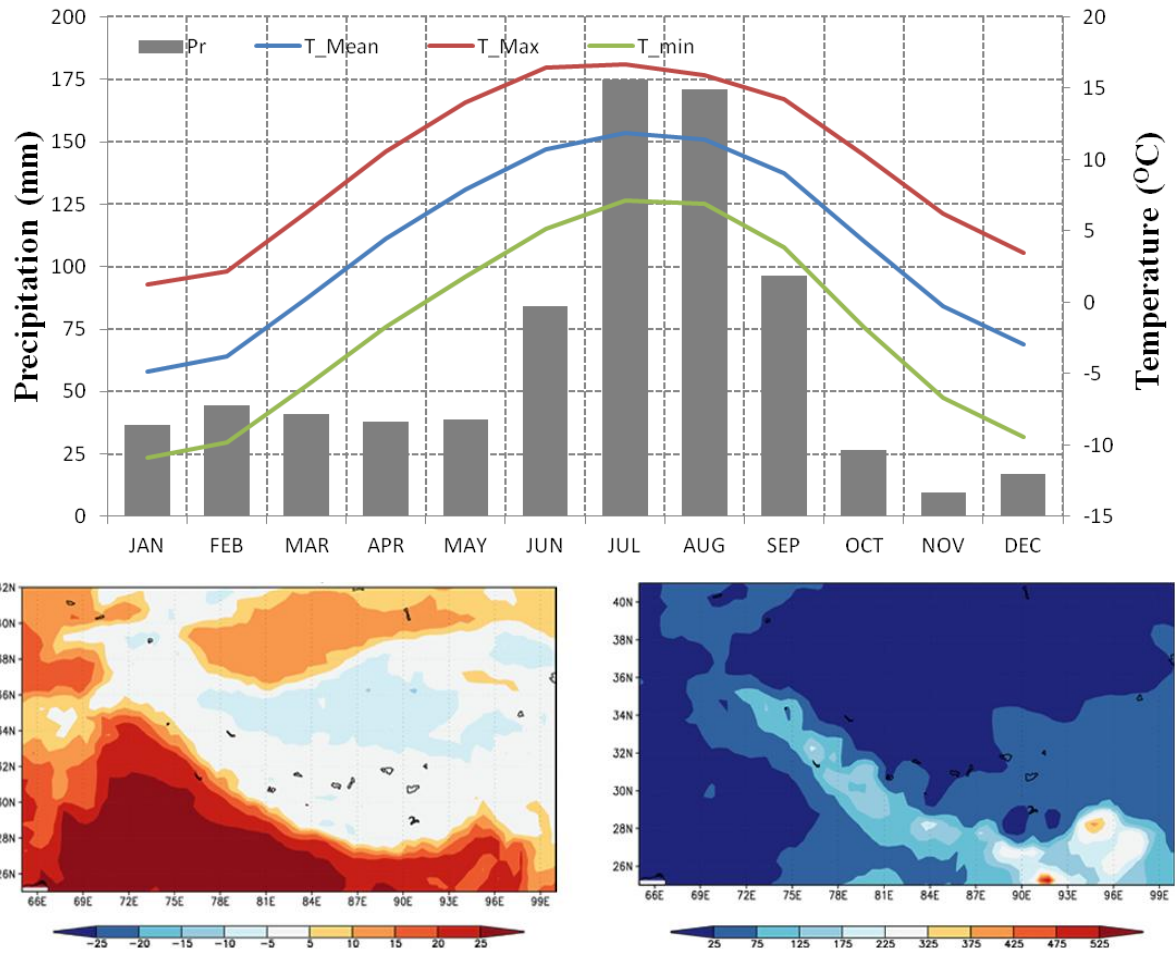
Figure S2. **Regional climatology**. Upper panel: Annual mean meteorological condition in our study region (30.15° to 31.03° N and 78.78° to 80.73° E) as derived from regional meteorological stations and reanalysis dataset (CRU-TS 4.01, 1901-2016; scale: 2.5º). (Pr: precipitation; T_Mean: mean temperature; T_Max: Maximum temperature; T_Min: Minimum temperature). Lower panel: Spatial trend of mean annual temperature (˚C) and mean annual precipitation (mm) (CRU-TS 4.01, 1901-2016).
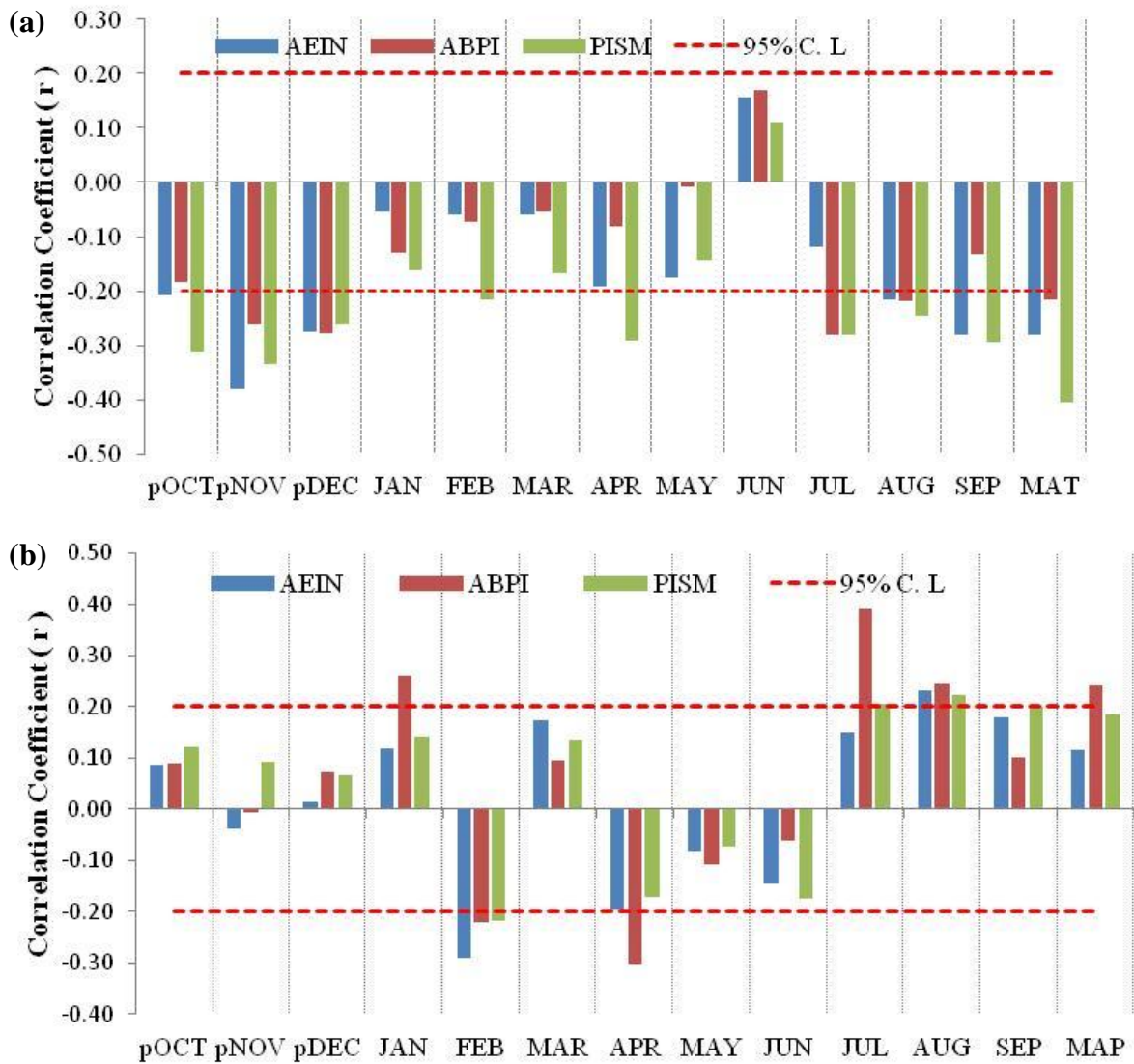
Figure S3. **Climate-response function**. Correlations between $\delta^{13}C$ chronologies with (**a**) mean monthly temperature; and (**b**) total monthly precipitation. Blue, Red and Green bars represent the correlations value with *Abies pindrow* (ABPI), *Picea smithiana* (PISM), and *Aesculus indica* (AEIN). The red dotted horizontal line indicates the 95% confidence level. Prefix '*p*' before the months denotes the months of the previous growth year.

(a)

(b)

R² = 0.465
Adj R² = 0.44
RMSE = 0.152
Intercept = 8.45
Slope = 0.384
P = 0.0003367
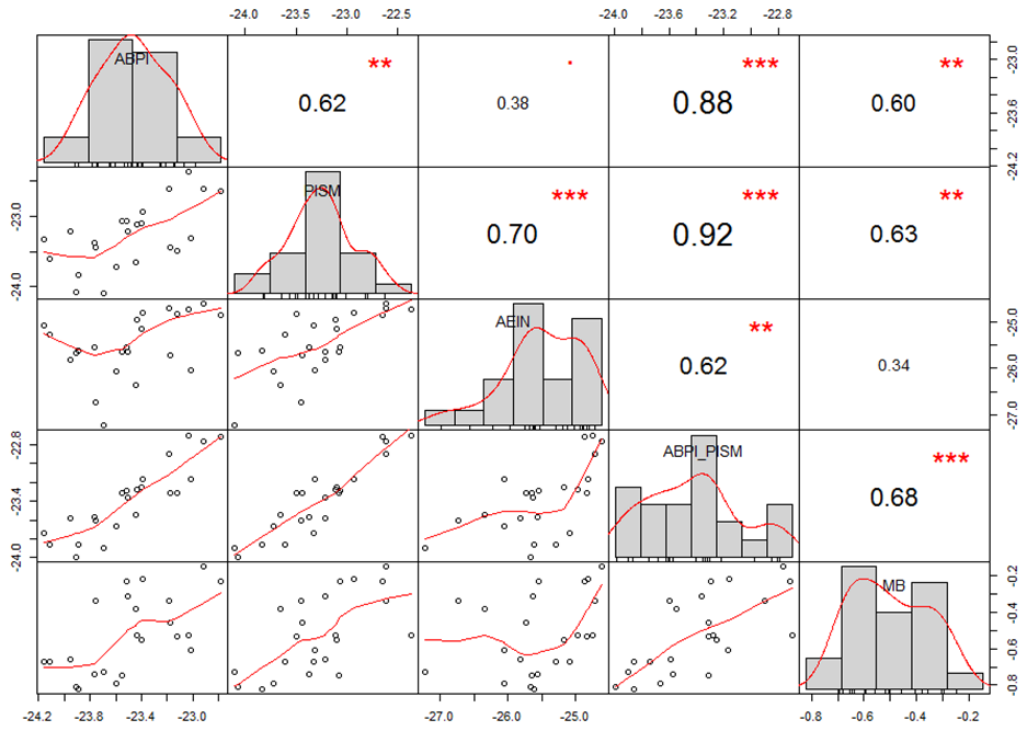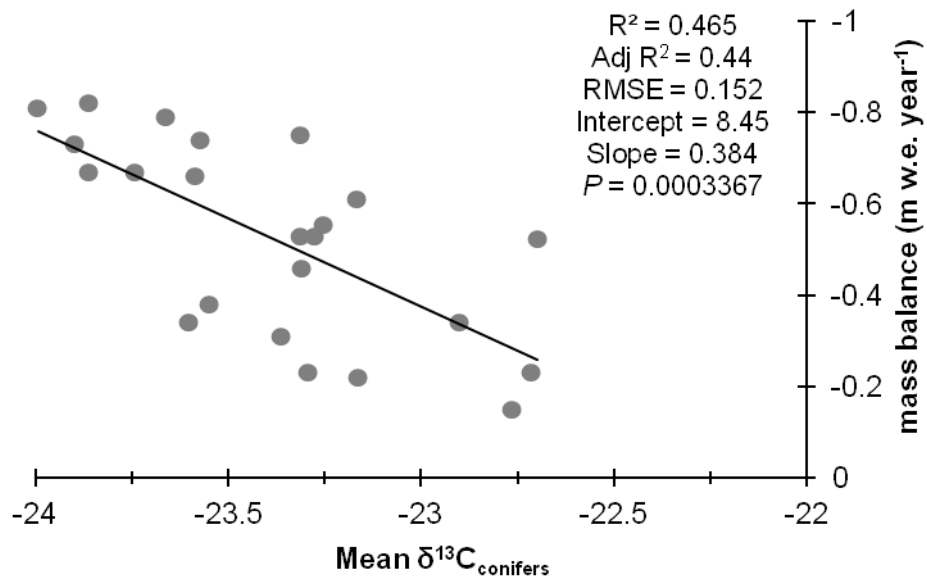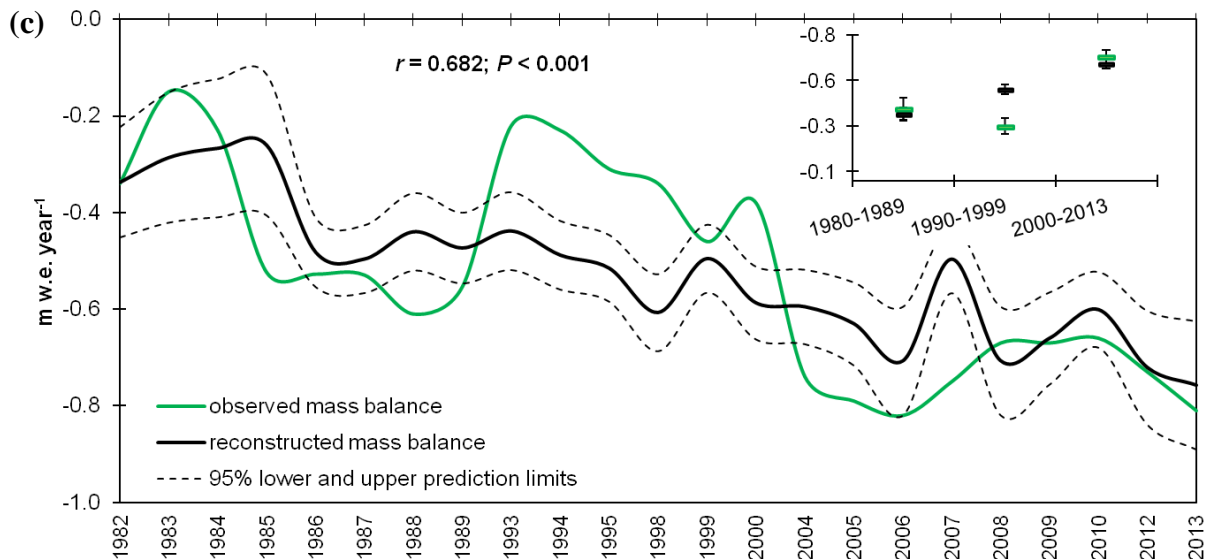
Figure S4. **Correlation matrix of species δ¹³C chronologies and mass balance** (**a**) The correlation matrix and pair plots of δ¹³C chronologies of conifers (*Abies pindrow*: ABPI; *Picea smithiana*: PISM), broadleaf deciduous (*Aesculus indica*: AEIN) and Mass Balance (MB). The distribution of each variable is shown on the diagonal. On the bottom of the diagonal bivariate scatter plots with a fitted line are displayed and on the top value of the correlation plus the significance levels have been indicated (*p*-values: 0.01*; 0.05**; 0.001***). (**b**) Scatter plot of mean δ¹³C chronology of conifers (ABPI-PISM) and MB with a linear relationship highlighted for 23 years: 1982-2013 (having gap years of: 1990-1992, 1996, 1997, 2001-2003 and 2011). (**e**) Comparison plot of observed and reconstructed mass balance. Inset plot indicates decadal coherence. Low coherence in the 1990s could be ascribed to relative gap in *in-situ* mass balance measurements.

(a)

(b)

(c)

(d)

(e)
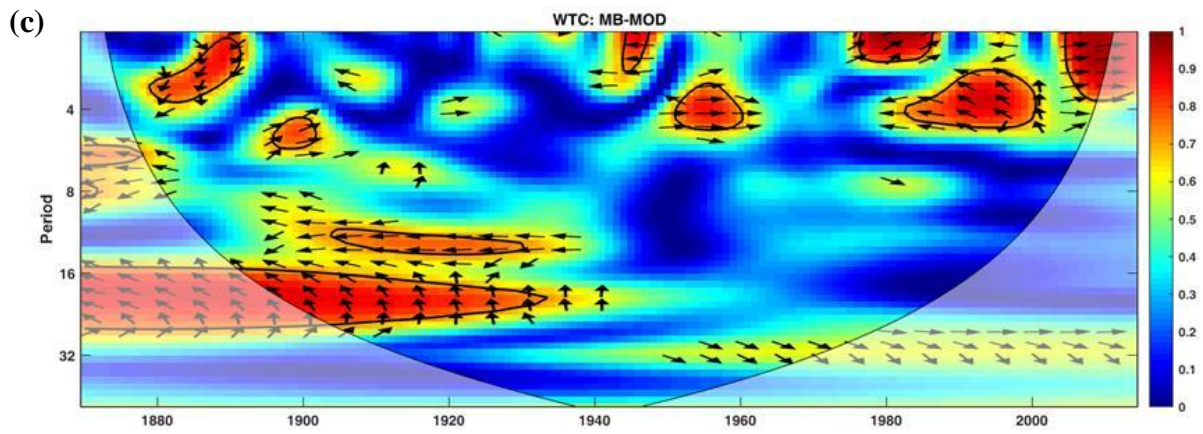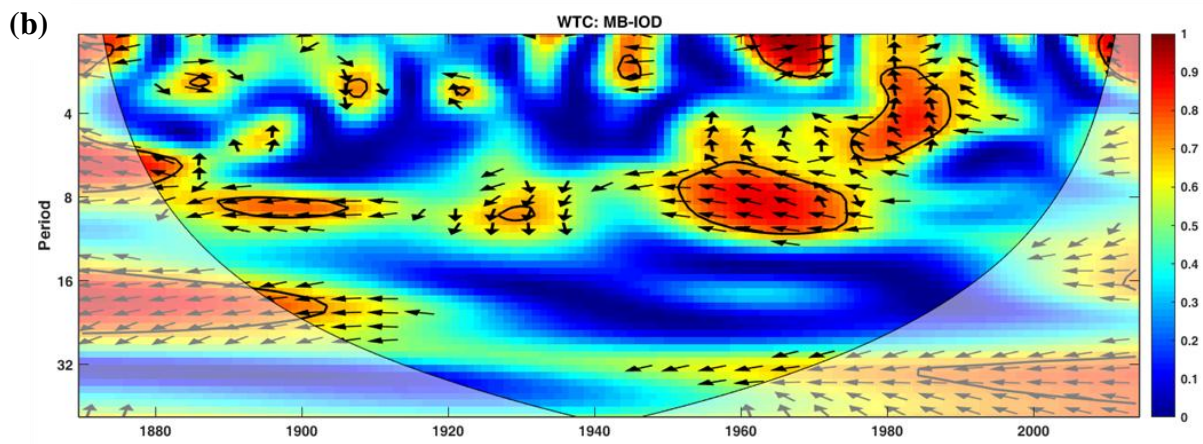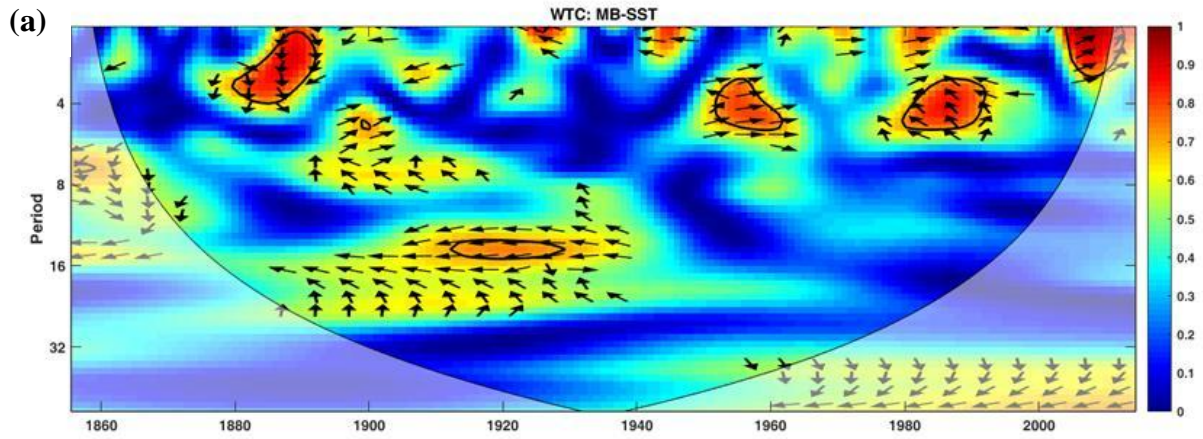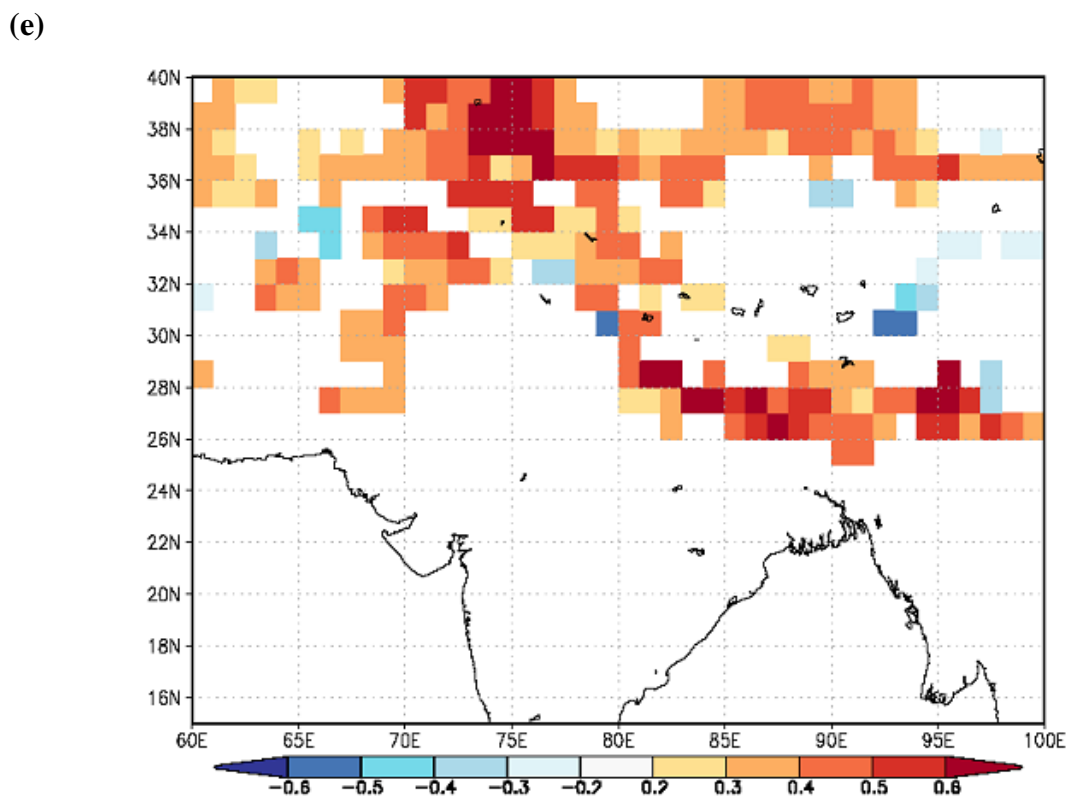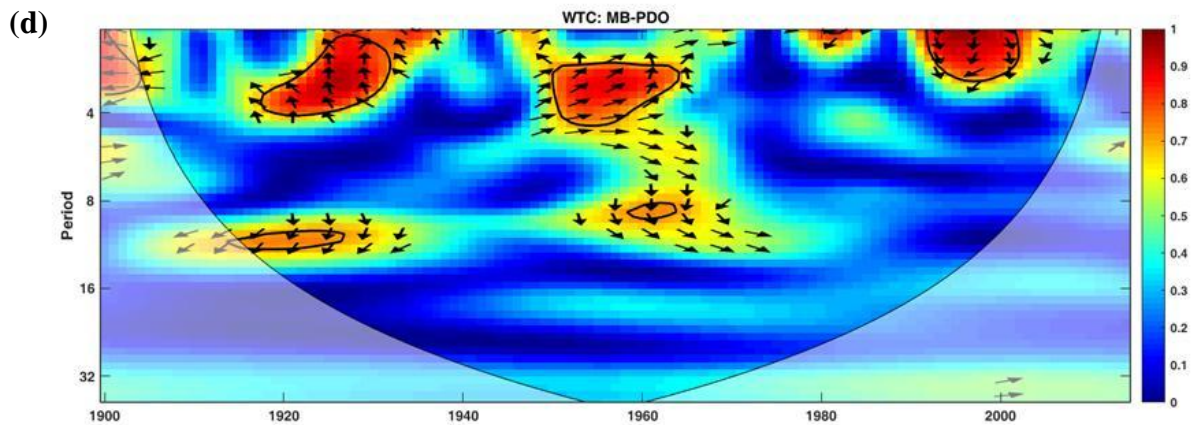
Figure S5. **Climate and mass balance coherence analyses**. Squared wavelet coherence between the standardized mass balance (MB) time series and (**a**) Nino4 SST, (**b**) Indian Ocean Dipole (IOD), (**c**) ENSO Modoki (MOD), and (**d**) Pacific Decadal Oscillation (PDO). The 5% significance level against red noise is shown as a thick contour. The relative phase relationship is shown as arrows (with in-phase pointing right, anti-phase pointing left, and indices leading MB by 90º pointing straight down and vice versa. The observations indicate that the phase angles are variable across the scales and denote a variable time lag between MB and indices arising due to temporally variable signal propagation. Arrows pointing upwards suggest that SST slightly leads MB. However, high circular standard deviation indicates a high variability and fades any firm conclusion on a stronger SST-MB link. (**e**) Spatial correlation map between annual snow cover data (NOAA: 1966-2013) and reconstructed MB. The map is generated using the KNMI Climate Explorer (http://climexp.knmi.nl)
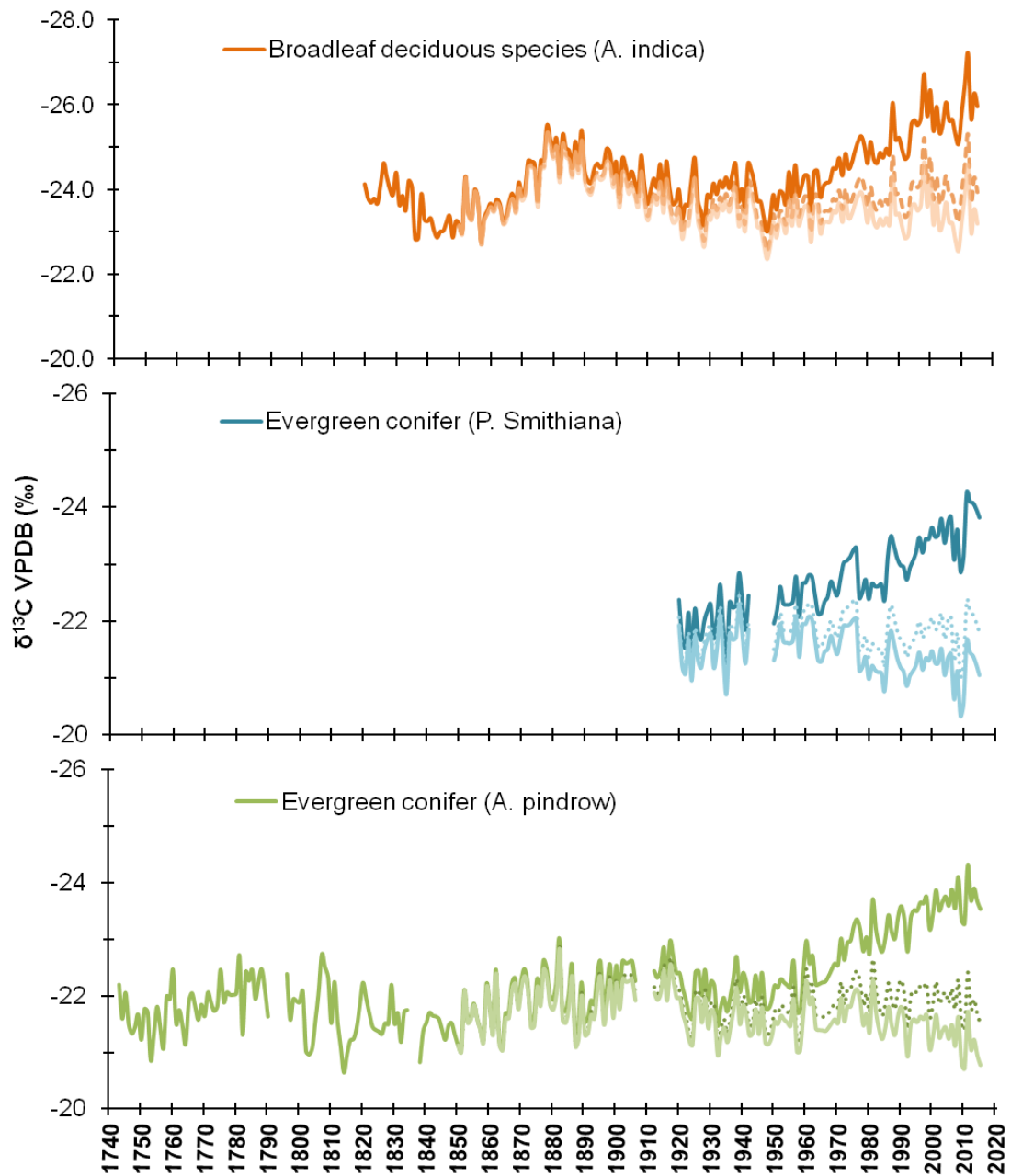
Figure S6. Atmospheric CO_2 effect on species' $\delta^{13}C$ chronologies. Comparison of raw $\delta^{13}C$ series (dark lines), $\delta^{13}C$ series corrected for post-industrial changes in the isotopic composition of atmospheric CO_2 (dotted lines), and $\delta^{13}C$ series after additional correction for the physiological responses to increasing concentrations of atmospheric CO_2 (bright lines) for the broad-leaf deciduous species (*Aesculus indica*), and for two evergreen conifer species (*Picea smithiana* and *Abies pindrow*).

Table S1: Descriptive statistics of δ¹³C chronologies of three tree species from DOK glacier valley region

	Aesculus indica (AEIN)	*Abies pindrow* (ABPI)	*Picea smithiana* (PISM)
Chronological years	1820 - 2015 (196 yrs)	1743 - 2015 (273 yrs)	1920 - 2015 (96 yrs)
Mean ± Std. error (‰)	-24.31 ± 0.05	-22.19 ± 0.04	-22.72 ± 0.06
Std. deviation (‰)	0.82	0.7	0.65
Coefficient of variation (%)	3.4	3.2	2.8
First-order autocorrelation	0.81	0.8	0.86
Inter-tree correlation (1976-2015)	0.5 - 0.83	0.6 - 0.87	0.62 - 0.83
Inter-species correlation (common period)	0.818 (AEIN - ABPI)	0.843 (ABPI - PISM)	0.824 (PISM - AEIN)
Annual phenology	Broadleaf deciduous (April-September)	Evergreen conifer	Evergreen conifer

Table S2. Glacio-morphological characteristics of four benchmark glaciers in the central Himalaya, India (2015)

Sl. No.	Name of the Glacier	Lat/Lon	Area (km^2)	Length (km)	Debris covered area (%)	Altitudinal range (m asl)	Aspect	Observed mass balance period (gap year)	Mean mass balance (m w.e. yr^{-1})	SLA (m asl)	Retreat (m/y) 1994-2015	Deglaciation (%) 1994-2015	Mean slope (º)	AAR	Velocity (m/yr)	Reference
1.	Chorabari (CHO)	30°74' N 79°09'E	5.63	7.2	25	6034 - 3866	N	2004 - 2013 (2011)	−0.73	3852	7.36 ± 2.45	3.60 ± 1.48	25.70	0.53	14.50	Pratap et al., 2015; Garg et al. (2017), (2019)
2.	Dokriani (DOK)	30°50' N 78°50'E	6.34	5.77	15	6120 - 3985	NW	1993 - 2000 (1996- 1997)	−0.32	3979	18.30 ± 2.49	2.46 ± 1.94	24.78	0.55	11.41	Pratap et al., 2015; Garg et al. (2017), (2019)
3.	Dunagiri (DUN)	30°33' N 79°54'E	2.25	5.93	75	5278 - 4374	N	1985 - 1989	−1.04	4374	6.10 ± 2.45	3.48 ± 3.88	12.27	0.13	--	Pratap et al., 2015; Garg et al. (2017), (2019)
4.	Tipra Bamak (TIP)	30°44' N 79°41'E	5.47	7.48	55	5422 - 3835	NW	1982 - 1989	−0.14	3836	17.78 ± 2.45	4.20 ± 1.29	18.52	0.23	9.42	Pratap et al., 2015; Garg et al. (2017), (2019)

Table S3. Statistics of calibration, and leave-one-out cross-validation (LOOCV) for annual mass balance reconstruction

Model calibration statistics: r = + 0.6821; R-squared: 0.4653; Adjusted R-squared: 0.4398; F-statistic: 18.28; $P < 0.0001$; RMSE: 0.159; and DW: 1.17.

leave-one-out cross-validation (LOOCV)

	r	R^2	F	Sign test (+/-)	PMT	RMSE	RE	CE	DW
GMB	0.609**	0.371	12.371**	$14^+/9^-$	4.01	0.166	0.364	0.364	1.21**

r: correlation coefficient; R^2: explained variance; F: F-test, Sign-test sign of paired observed and estimated departures from their mean on the basis of the number of agreements/disagreements; Product Mean Test (PMT) is the PMT is the product mean T statistics, RMSE: root mean squared error; RE: reduction of error; CE: coefficient of efficiency; DW: Durbin–Watson test; *$p < 0.05$, **$p < 0.001$

Table S4. Correlation among species δ¹³C chronologies and Mass Balance

	Correlation Coefficient (r)	P value
MB vs. ABPI	0.596	2.68e-03
MB vs. PISM	0.631	1.25e-03
MB vs. AEIN	0.343	1.09e-01
MB vs. ABPI-PISM	0.682	3.36e-04
ABPI vs. PISM	0.843	1.52e-03
ABPI vs. AEIN	0.818	2.69e-02
PISM vs. AEIN	0.824	1.37e-04
ABPI vs. ABPI-PISM	0.881	2.88e-08
PISM vs. ABPI-PISM	0.919	6.40e-10
AEIN vs. ABPI-PISM	0.617	1.72e-03

(*Abies pindrow*: ABPI; *Picea smithiana*: PISM; *Aesculus indica*: AEIN; Mass Balance: MB).

Table S5. Correlation between species $\delta^{13}C$ chronologies and monthly meteorological data

	Temperature (^{o}C)				Precipitation (mm)		
Months	AEIN	ABPI	PISM	Months	AEIN	ABPI	PISM
pOCT	-0.207	-0.184	-0.313	pOCT	0.086	0.088	0.121
pNOV	-0.380	-0.260	-0.333	pNOV	-0.036	-0.007	0.091
pDEC	-0.273	-0.278	-0.261	pDEC	0.012	0.073	0.065
JAN	-0.053	-0.128	-0.162	JAN	0.119	0.262	0.141
FEB	-0.060	-0.073	-0.215	FEB	-0.289	-0.221	-0.216
MAR	-0.060	-0.053	-0.168	MAR	0.174	0.094	0.137
APR	-0.190	-0.079	-0.292	APR	-0.195	-0.302	-0.172
MAY	-0.176	-0.008	-0.144	MAY	-0.081	-0.106	-0.072
JUN	0.1572	0.1691	0.109	JUN	-0.144	-0.060	-0.173
JUL	-0.119	-0.279	-0.279	JUL	0.149	0.390	0.206
AUG	-0.215	-0.219	-0.246	AUG	0.232	0.245	0.223
SEP	-0.281	-0.131	-0.292	SEP	0.178	0.101	0.201
Annual	-0.281	-0.215	-0.405	**Annual**	0.115	0.243	0.185

(*Abies pindrow*: ABPI; *Picea smithiana*: PISM; *Aesculus indica*: AEIN; prefix 'p' before the months denotes the months of the previous growth year)

Table S6: Correlation between regional tree-ring δ^{18}O with three species from DOK glacier valley region (Uttarakashi) $P < 0.05$)

Uttarakashi	Manali	Jageswar	Humla	Ganesh	Bhutan
Abies pindrow (Evergreen conifer)	0.75	0.67	0.23	0.20	0.26
Picea smithiana (Evergreen conifer)	0.69	0.56	0.50	0.52	0.26
Aesculus indica (Deciduous broadleaf)	0.60	0.55	0.50	0.57	0.31